



**HAL**  
open science

## Oxidative pyrolysis of wood chips and of wood pellets in a downdraft continuous fixed bed reactor

Elias Daouk, Laurent van De Steene, Frederic Paviet, Éric Martin, Jeremy Valette, Sylvain Salvador

### ► To cite this version:

Elias Daouk, Laurent van De Steene, Frederic Paviet, Éric Martin, Jeremy Valette, et al.. Oxidative pyrolysis of wood chips and of wood pellets in a downdraft continuous fixed bed reactor. *Fuel*, 2017, 196, pp.408-418. 10.1016/j.fuel.2017.02.012 . hal-01619256

**HAL Id: hal-01619256**

**<https://hal.science/hal-01619256>**

Submitted on 30 Mar 2018

**HAL** is a multi-disciplinary open access archive for the deposit and dissemination of scientific research documents, whether they are published or not. The documents may come from teaching and research institutions in France or abroad, or from public or private research centers.

L'archive ouverte pluridisciplinaire **HAL**, est destinée au dépôt et à la diffusion de documents scientifiques de niveau recherche, publiés ou non, émanant des établissements d'enseignement et de recherche français ou étrangers, des laboratoires publics ou privés.

# Oxidative pyrolysis of wood chips and of wood pellets in a downdraft continuous fixed bed reactor

Elias Daouk<sup>a,b,c,\*</sup>, Laurent Van de Steene<sup>a</sup>, Frederic Paviet<sup>c</sup>, Eric Martin<sup>a</sup>, Jeremy Valette<sup>a</sup>, Sylvain Salvador<sup>b</sup>

<sup>a</sup> CIRAD – UR BioWooEB, 73 Avenue Jean-François Breton, 34398 Montpellier Cedex 5, France

<sup>b</sup> RAPSODEE, CNRS UMR 5203, Mines-Albi, Campus Jarlard, 81013 Albi Cedex 09, France

<sup>c</sup> GEPEA, UMR 6144 CNRS, Université de Nantes, Ecole des Mines de Nantes, ENITIAA, DSEE, 4 rue Alfred Kastler, BP 20722, 44307 Nantes Cedex 3, France

## Keywords:

Oxidative pyrolysis  
Fixed-bed  
Biomass  
Smoldering  
Yields of products

## H I G H L I G H T S

- A counter-current oxidation zone was stabilized inside a downdraft reactor.
- Detailed mass balance including char, permanent gases and tar yields.
- The fed air flow rate and the fuel (wood) density were varied.
- Insights acquired on the shape and stability of the oxidation zone.

## A B S T R A C T

In air staged gasification and advanced carbonization processes, oxidative pyrolysis occurs in downdraft continuous fixed bed reactors. An oxidation zone separates the virgin fuel from the resulting char and propagates upward. Here, the oxidation zone was stabilized at a fixed elevation in a 20 cm I.D. fixed bed reactor using wood chips or wood pellets. In controlled continuous operating mode, we investigated the impact of air flux and bed bulk density on the behavior of the oxidation zone in terms of wood consumption, and yields of char, gas and tars. An air:wood mass ratio of 0.7 was measured and in our operating conditions, and was not sensitive to air mass flux and bed density. With oxidative pyrolysis, yields of organic condensates were lower than with allothermal pyrolysis, whereas the production of pyrolysis water and permanent gases increased. Finally, the oxidation zone was shown to be flat and horizontal in a wood pellet bed but inclined in a wood chip bed.

## 1. Introduction

Thermochemical biomass conversion, i.e. combustion, gasification, and pyrolysis, can convert a biomass into useful energy such as heat, electricity, or liquid fuel. Although biomass combustion has clearly reached the commercial development stage, the trajectories of the two other routes are quite different.

Pyrolysis was widely developed for charcoal production, also called carbonization, in the past, but in most cases, the technologies remain simple and robust and not always adapted to the need for efficiency and environmental constraints today [1]. Nevertheless thanks to the awareness of some constructors, but also due to the new interest in charcoal as reducing agent, fertilizer, or

active carbon, the technologies have been significantly improved in recent years.

Research and development programs on gasification have been underway for many years; some commercial demonstrations exist, but the technology positioning in the market remain fragile and the success stories still limited [2]. Nevertheless, a wide range of reactors have been developed varying mainly in their feedstocks and applications. Usually, a simple classification is proposed based on the size of the installation: entrained flow, fluidized bed, and fixed bed reactor, for large, medium and small reactors, respectively. Fixed bed reactors are widely acknowledged to be the best solution for low power production because of their greater simplicity and lower production cost.

In many of the above mentioned carbonization and small scale staged gasification processes, biomass pyrolysis occurs in a specific continuous downdraft fixed bed configuration. But in the same way as in any thermochemical conversion processes, pyrolysis plays a major role as it produces char and pyrolysis gases that

\* Corresponding author at: CIRAD – UR BioWooEB, 73 Avenue Jean-François Breton, 34398 Montpellier Cedex 5, France.

E-mail address: [elias.daouk@mines-albi.fr](mailto:elias.daouk@mines-albi.fr) (E. Daouk).

are subsequently converted. Moreover, partial oxidation can be a simple and efficient way to sustain pyrolysis, by providing the energy needed for heating, drying, and endothermic reactions of the conversion, and to allow the process to be autothermal: it is thus referred here as oxidative pyrolysis.

During pyrolysis in continuous downdraft reactors, the biomass and air are fed into the top of the reactor and char and pyrolysis gases are removed from the bottom. We define the oxidation zone as the reactive zone inside the packed bed where major changes in temperature and gas composition take place (Fig. 1). This zone separates the unreacted biomass from the char and is the location of several complex and coupled transformations or reactions. The first to occur is drying. When the temperature increases, oxidative pyrolysis occurs, which can be defined as a combination of biomass oxidation and biomass pyrolysis [3]. Then, oxidation of some light and heavy pyrolysis gases, and of char, provides the energy to the system, and thus allows the propagation of the oxidation zone.

The stabilization of the oxidation zone inside the bed is of particular interest for operators because (i) the top of the bed is maintained at a low temperature, thereby facilitating control of the process and limiting the production and deposition of tar, and (ii) a higher temperature zone is created that favors tar cracking when crossing it.

The upward propagation of the oxidation zone towards the virgin biomass can be controlled by removing char from the bottom of the reactor, which causes a downward movement of the whole bed.

The propagation of an oxidation zone in a porous medium, called smoldering, has been studied in many contexts, including forest fires and tree trunk combustion [4,5], home fires and burning of polymeric foams or tissue [6], propagation of underground fires in coal mines [7] or in oil shale exploitation [8], organic waste incineration [9,10], and also during combustion of cigarettes [11]. These configurations differ in several respects. In particular the two first examples [4–6] refer to natural smoldering, as opposed to forced smoldering [7–11], which describes situations where the air flow is forced to cross the porous media, as in packed bed incineration and oil shale combustion. Moreover, forced smoldering is classified as reverse (counter-current) or forward (co-current) depending upon the relative directions of the air and of the propagation of the oxidation zone in the porous medium. In forward smoldering [7,8,11] the oxidation zone moves in the same direction as the air flow. In reverse smoldering, it propagates in the opposite direction to that of the air mass flux, meaning that air first crosses the unreacted carbonaceous material [9,10,12–14].

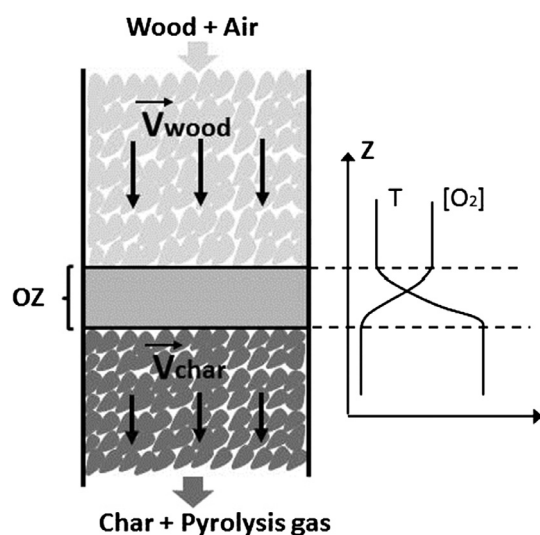


Fig. 1. Oxidative pyrolysis in a continuous downdraft fixed bed reactor.

The oxidative pyrolysis of wood chips in a continuous fixed bed investigated here involves forced reverse smoldering because oxidation zone propagates upwards, in opposite direction to wood and air flows [15].

In smoldering, the oxidation zone can be described by several specific features: - its propagation rate; - its temperature; - its geometry, thickness and shape; - its yield of char, gases, and tar, and the composition of these outputs. These features can be observed experimentally using the appropriate research equipment. Their prediction remains a real challenge for researchers, as they require the elaboration of complex models combining a description of chemical reactions with heat and mass transfer phenomena.

Among these features, the propagation rate of the oxidation zone has been widely investigated in the literature on reverse smoldering [10–15]. It should be noted here that when referring to propagation rate or velocity, the terms “front” or “ignition front” are more commonly used by authors than oxidation zone. The propagation rate, which is controlled by combustion and heat and mass transfers, depends on: - air flow-rate; - fuel properties like size, density, thermal conductivity, moisture, volatile matter, ash, and elemental composition; - and bed properties, such as porosity and density. However, as mentioned by Mahapatra and Dasappa [12], not all of these parameters are independent variables and most are interrelated, so that drawing conclusions about the dependence of each separate parameter on the behavior of the oxidation zone is very difficult.

Nevertheless, there is a consensus in the literature that air mass flux is the parameter that has the most influence on the propagation rate. This point has been checked on more than 10 carbonaceous feedstocks with significantly different properties [13,16]. Regarding the influence of the air mass flux, the propagation rate inside a wood packed bed initially increases as the air mass flux increases until it reaches a peak. A further increase in the air mass flux then results in a decrease of the propagation rate. Three different regimes are usually identified in reverse smoldering applied to the combustion process, which are determined by the main process controlling the propagation of the front: oxygen-limited, reaction limited and quenching by convection [13,16,17].

Air mass flux does not only influence the propagation rate, but also the other features of the oxidation zone. It has been shown that peak temperature in the zone increases with an increase in the air flux until a maximum is reached in the sub-stoichiometric conditions of the combustion regime [13]. An increase of about 100 °C in temperature has been reported when air mass flux fed through a wood downdraft batch gasifier was increased from 0.12 to 0.14 kg m<sup>-2</sup> s<sup>-1</sup> [12]. In these studies, these maximum temperatures match the maximum propagation rates of the oxidation zone.

Regarding geometry, some authors have attempted to measure the thickness of the ignition zone in counter current combustion processes. It has been reported to be in the same order of magnitude as particle size [14,16], and is said not be sensitive to the air flux [14].

The influence of the biomass or bed properties has been more rarely investigated. But the few studies that did showed that front propagation velocity was higher when: - particle size [13,16,17] or water content [10,13,17] or ash content [13] was low; or - when the heating value [13,17] was high. Moreover, ignition front speed was shown to be inversely proportional to bed bulk density [16,18].

From the previous literature on reverse smoldering, the following remarks can be made. First, most of the studies focused on understanding the propagation rate. Other specific features of the oxidation zone received less attention, in particular, the geometry of the oxidation zone and yields and the composition of all the products leaving this zone. Second, very little information is available on the influence of operating parameters and fuel/bed properties on the features of the whole oxidation zone, and more

quantitative results would be useful to enhance our understanding. And finally, all previous works mentioned here were performed under batch conditions, and, all except one [12], involve a downdraft movement of the oxidation zone. Thus, reverse smoldering in a continuous downdraft fixed bed reactor has never been specifically investigated.

This research report focuses on the oxidative pyrolysis of wood in a continuous fixed bed reactor, characterized by a downward reverse smoldering configuration. The objective of the study was to quantify the impact of two parameters of major importance: the air mass flux and the bulk density of the packed bed, on the features of the oxidation zone. We focus on the measurement and observation of the following specific features of the oxidation zone: - yields and the composition of char, gas, and tar produced; - and its shape.

Results of this study give a new insight on reverse smoldering in continuous downdraft fixed bed reactors. Data provided could be useful for researchers for the validation or development of CFD models. Regarding applicability, the works presented provide a better understanding of the behavior of the oxidative pyrolysis stage in staged fixed-bed gasification or carbonization processes and may support constructors and operators in optimization of their process design and operation.

The experimental results presented in this paper were obtained in a stationary regime. The oxidation zone was stabilized at a given elevation in a continuous downdraft fixed bed reactor with different air mass fluxes and bed densities. The air mass fluxes were selected in a range appropriate for the oxidative pyrolysis step of air staged gasifiers. We tested two types of wood, chips and pellets, which differ considerably in particle size and density, both of which are of major interest for different applications.

## 2. Experimental device and procedures

### 2.1. Description of the reactor

A continuous fixed bed reactor (CFiBR) developed by CIRAD was used for this study. This reactor was originally designed to study char gasification [19–21]. Later on, Milh e et al. [15], adapted the reactor to study the auto-thermal and allothermal pyrolysis of wood chips. Fig. 2 shows the experimental setup. It is mainly composed of the reactor tube, the feeding system and the extraction system. The reactor tube, made of refractory stainless steel, has an internal diameter of 20 cm and is 160 cm long. It is equipped with eight tapping pipes with 1 mm thermocouples fitted lengthwise to the reactor at 10 cm intervals. A sampling pipe is located in the lower part of the reactor to collect gases at the outlet. Wood particles are supplied through the top of the reactor via a 2 m long conveyor belt and two pneumatic valves that act as an airlock. Wood particles are supported by a grid at the bottom of the reactor to form a fixed bed at a height of about 80 cm. The height of the bed is controlled by a laser beam device connected to the feeding system. Energy to support front propagation is supplied by air injected through the top of the reactor to feed the oxidation zone (OZ) in the bed. Wood is converted to char, tars and gases. Char is removed from the bottom of the reactor manually using a scraper, while all the gases flow through a heated pipe to a post-combustion chamber via a cyclone to separate the fines.

### 2.2. Sampling train

Fig. 3 shows the sampling train designed to measure the tar and the permanent gas flow rates together with their compositions. The sampling train is connected to the reactor via the sampling pipe located below the grid supporting the fixed bed. Gaseous

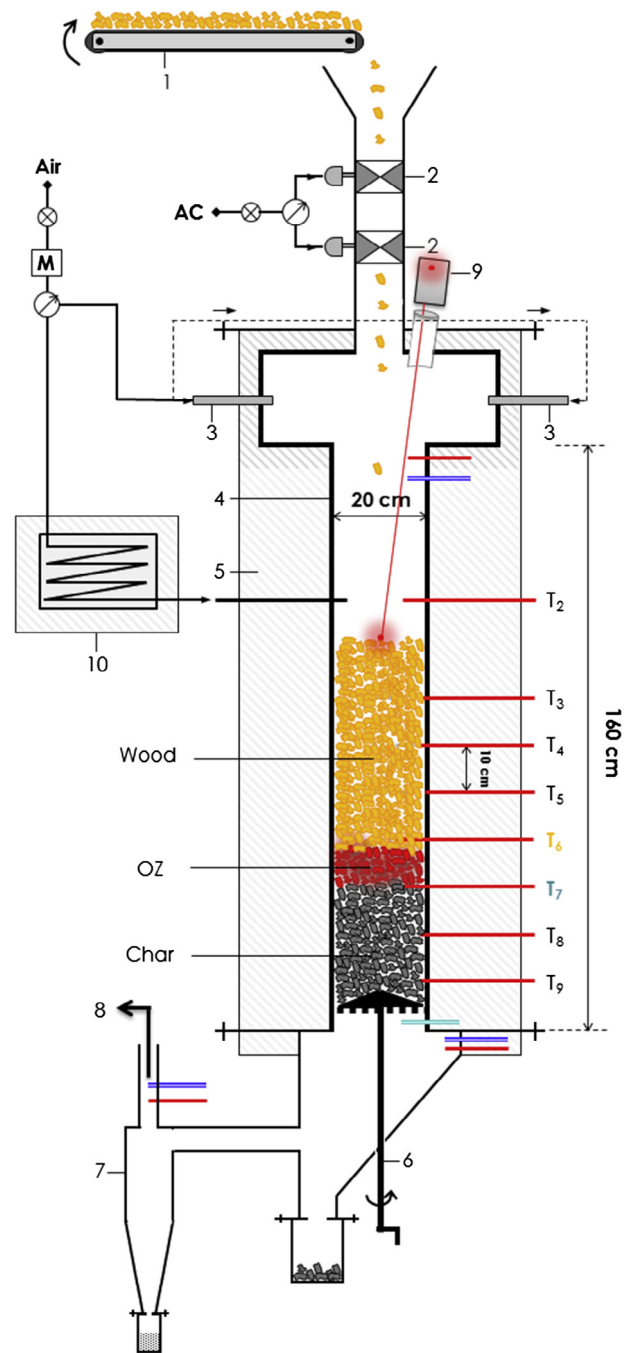
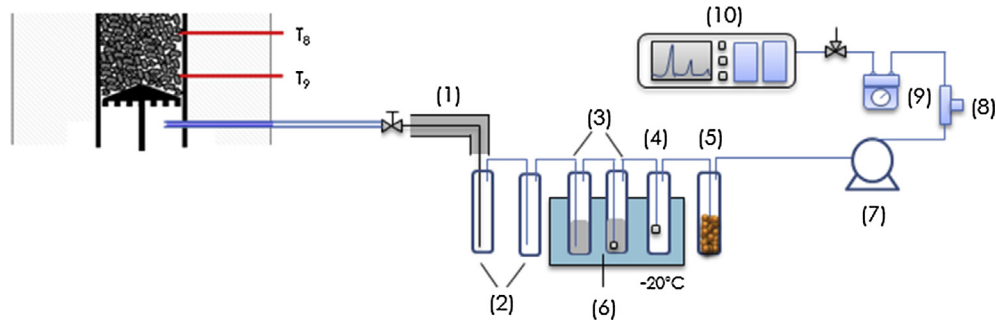
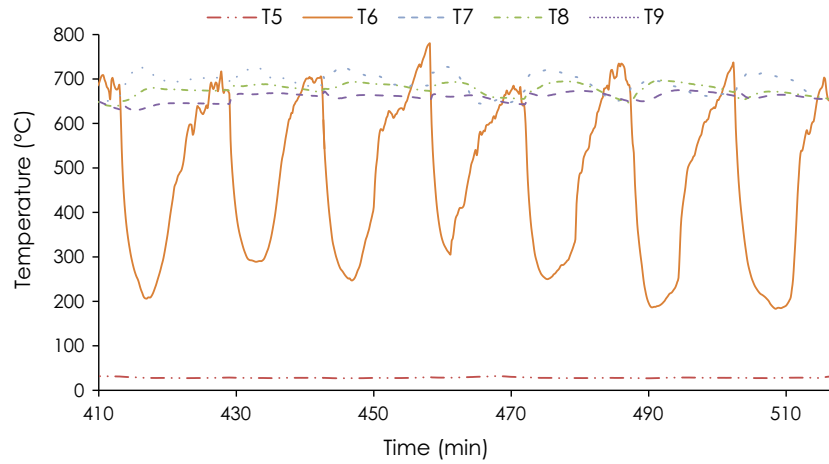


Fig. 2. Schematic diagram of the CFiBR. (1) Conveyor, (2) airlock, (3) fresh air supply, (4) reactor tube, (5) insulation, (6) char removal device, (7) cyclone, (8) to post combustion, (9) laser, (10) air preheater.

products first flow through a series of 6 impingers. The first two are empty and at ambient temperature; the water can condensate to prevent plugging due to water freezing in the cold bath. The following three are immersed in a bath cooled to about  $-20\text{ }^{\circ}\text{C}$ . The first contains isopropanol; the second also contains isopropanol but is also equipped with quartz frit, while the third is only provided with a quartz frit. The last impinger is filled with silica gel to trap the last traces of water and to protect the downstream gas analyzer. The gas then successively passes through the pump, the gas flow meter, and a micro-gas chromatography system (micro-GC). The latter is equipped with two columns to measure the concentrations of permanent gases ( $\text{N}_2$ ,  $\text{O}_2$ ,  $\text{CO}$ ,  $\text{CO}_2$ ,  $\text{H}_2$ ,  $\text{CH}_4$ ,  $\text{C}_2\text{H}_4$  and  $\text{C}_2\text{H}_6$ ) at the gas outlet.



**Fig. 3.** Sampling train. (1) heated conduit, (2) empty impingers, (3) isopropyl alcohol impingers, (4) quartz frit impinger, (5) silica gel impinger, (6) cold bath at  $-20^{\circ}\text{C}$  (7) pump, (8) flow meter, (9) gas meter, (10) micro-GC.



**Fig. 4.** Temperatures recorded by thermocouples  $T_5$  to  $T_9$  during an experiment with wood chips and minimum air flow rate.

### 2.3. Operating mode

#### 2.3.1. Starting step

In autothermal pyrolysis experiments, the heat necessary to dry and pyrolyze the wood chips is supplied by combustion in the so called “oxidation zone” in the fixed bed. First, the oxidation zone is ignited at the surface of a thin layer char bed at the bottom of the reactor by an external energy source and ambient air is injected at the top of the reactor at a sufficiently high flow rate to maintain combustion. In our experiment, the external energy source consisted in some burning barbecue-lighter particles dropped onto the surface of the layer of charcoal. After ignition of the oxidation zone, the air flow rate from the top of the reactor was reduced to the value to be investigated in the test, and the reactor was filled with wood chips or wood pellets to a height of about 80 cm from the bottom grate. The oxidation zone then spreads upward. The rise in the OZ is monitored by observing the increase in the temperature measured along the bed. When the OZ reaches the height required for the test, it is maintained more or less still, as described below.

#### 2.3.2. Control of the oxidation zone inside the fixed bed

The main challenge of this type of experiment is keeping the oxidation zone at a fixed elevation while continuously feeding wood and removing char. In our case, we chose an oxidation zone close to the middle of the total height of the solid bed, i.e. 35 cm above the grid holding the bed, where thermocouple T6 was positioned (Fig. 4). When the temperature recorded by T6 increased and reached the same value as the thermocouple positioned 10 cm below (T7), we manually extracted char from the bottom of the reactor. The OZ then descended a few millimeters in the

reactor due to the downward movement of the fixed bed. Thermocouple T6 recorded a sudden drop when it again came into contact with cold biomass. Next, the OZ rose again in the reactor. When the temperature recorded by T6 again reached the same value as T7, we extracted more char. Temperatures T7 to T9 varied slightly between  $650^{\circ}\text{C}$  and  $700^{\circ}\text{C}$ . Temperature T5, in the wood chips, remained constant at close to room temperature.

Because char is extracted and the bed compacted, total bed height decreases. The reactor has to be filled regularly to maintain a constant total bed height. To make this possible, a laser device was installed above the reactor to continuously measure the height of the bed. Fig. 5 shows the impact of bed compaction, char extraction, and wood reloading on the bed height during the course of the experiment. In this case, total bed height was between 65 and 72 cm. Wood reloading stopped automatically when the bed height reached the appropriate height and started again when the level dropped too low.

#### 2.3.3. Mass balance

Nitrogen from the introduced air ( $\dot{m}_{N_2,i}$ ) was used as a tracer to calculate the total mass flow rate of permanent gases ( $\dot{m}_{pg}$ ) at the outlet of the reactor according to Eq. (1):

$$\dot{m}_{pg} = \frac{\dot{m}_{N_2,i}}{Y_{N_2,o}} \quad (1)$$

$Y_{N_2,o}$ , which represent the nitrogen mass fraction in the permanent gases produced, was determined using the fraction measured by the micro-GC. The mass flow rates of each component ( $\dot{m}_{j,o}$ ) in the permanent gases in the outlet was calculated using the Eq. (2):

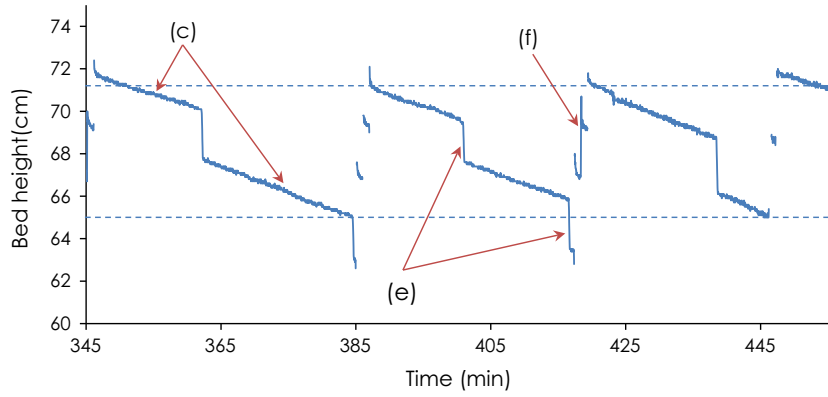


Fig. 5. Changes in bed height over the course of an experiment. (c) bed compaction, (e) char extraction, (f) wood filling.

Table 1

Repeatability of the mass balance for the experiment with wood chips and an air flux of  $0.022 \text{ kg m}^{-2} \text{ s}^{-1}$ . The difference is calculated relative to the inlets.

Flow rate (kg/h)		Test 1	Test 2	Test 3
Inlets	Wood	3.720	3.780	3.618
	Air	2.630	2.630	2.630
	Total	6.350	6.410	6.248
Outlets	Char	0.570	0.582	0.572
	Permanent gases	4.122	4.048	4.033
	Tars	0.297	0.247	0.304
	Water	1.263	1.111	1.250
	Total	6.252	5.988	6.159
	Difference	1.54%	6.58%	1.42%

$$\dot{m}_{j,o} = Y_{j,o} \dot{m}_{pg} \quad j = N_2, O_2, H_2, CO, CO_2, CH_4, C_2H_4, C_2H_6 \quad (2)$$

After sampling for about an hour, the impingers were weighed and the mass flow rate of sampled tars was calculated, assuming that the ratio of the tars to the permanent gas is the same in the total outlet gas as in the sampled gas (Eq. (3)):

$$\dot{m}_{t,o} = \dot{m}_{pg} \left( \frac{\dot{m}_{t,o}}{\dot{m}_{pg}} \right)_{\text{samp}} \quad (3)$$

The water mass fraction in the tars was determined using the Karl-Fischer technique.

Repeatability tests were performed for the experiment with an air flux of  $0.022 \text{ kg m}^{-2} \text{ s}^{-1}$ . The mass balances for the three experiments are listed in Table 1. A comparison of the mass flow-rates for each component of the three tests shows that repeatability was good. In addition, the mass balances were satisfactory. A maximum difference of 7% was measured between the masses of incoming and outgoing products. We can therefore consider that the methods used to determine the different mass-flow rates were reliable.

#### 2.4. Characteristics of the wood chips and wood pellets

Wood chips and wood pellets of maritime pine (*Pinus pinaster*) with bark were used for the experiments. Table 2 shows the results of proximate and ultimate analyses measured in compliance with standards. The wood chips and wood pellets can be considered similar in terms of composition. The bulk density for wood chips was  $220 \text{ kg/m}^3$  and around  $690 \text{ kg/m}^3$  for the wood pellets. The size distribution of the wood chips was determined by the horizontally oscillating screen method according to EN15149-1. Around 80 wt% of the wood chips were within the 1–8 mm size range. The cylindrical wood pellets were homogeneous in size, with a diameter of 6 mm of diameter and a length of around 20 mm.

Table 2

Ultimate and proximate analyses of the wood chips and wood pellets.

	Wood chips	Wood pellets
Moisture (wt%, w.b.)	9.8	8
<i>Proximate analysis (wt%, d.b.)</i>		
Ash	0.4	0.4
Volatile matter	83.7	83.3
Fixed carbon	15.9	16.3
<i>Ultimate analysis (wt%, d.b.)</i>		
C	49	51.7
H	7.2	7.1
N	0.1	0.1
O (by difference)	43.7	41.1
LHV (MJ/kg, d.b.)	18.3	19.1

### 3. Results and discussion

#### 3.1. Mass balances and yields

Results obtained in the reference conditions, i.e., wood chips as feedstock and an air flux of  $0.022 \text{ kg m}^{-2} \text{ s}^{-1}$ , are presented in this section. The mass balance and the distribution of the products between permanent gases, water, char and tars at the outlet are shown in Fig. 6, along with the composition of the permanent gases. The yield of each product was estimated as a percentage of the initial mass flow rate of dry wood chips. The total of measured yields is thus  $>100\%$ , as the oxygen mass introduced at the top of the reactor reacts in the bed and was recovered in the products. As the results are presented relative to initial dry wood, drying water was not included in the mass balance of outgoing products. Nitrogen, as an inert gas, was also removed from the mass balances.

In general, the mass balance at closure was satisfactory. The slight difference (around 6%) between the inlet and the outlet

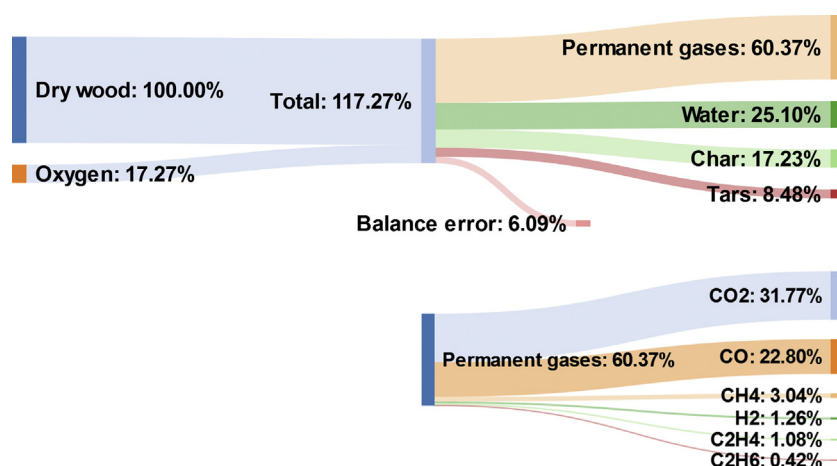


Fig. 6. Mass flow diagram of the experiment with wood chips and an air flux of  $0.022 \text{ kg m}^{-2} \text{ s}^{-1}$ . Yields are expressed in wt% relative to the initial dry wood.

can be attributed to errors in the calculation of flow rates for the solids, permanent gases, and tars.

In the case of wood chips, considering an air flux of  $0.022 \text{ kg m}^{-2} \text{ s}^{-1}$ , the corresponding wood flux is  $0.030 \text{ kg m}^{-2} \text{ s}^{-1}$ . The resulting yields of outgoing products were 17.2 wt% char, 25.1 wt% water, 8.5 wt% tars, and 60.4 wt% permanent gases.

These results show that the yield of tar from oxidative pyrolysis, 8.5 wt%, is very low compared to pyrolysis in inert atmosphere. In a previous study by the same research team [15], a tar yield of 31 wt% was measured during inert atmosphere pyrolysis at  $575 \text{ }^\circ\text{C}$  in the same fixed bed reactor. The low yields of tar during oxidative pyrolysis can be attributed to several reactions that may occur:

- Thermal cracking and oxidation in the oxidation zone, where the temperature is higher ( $700 \text{ }^\circ\text{C}$  for an air flux of  $0.022 \text{ kg m}^{-2} \text{ s}^{-1}$ ) than in the one during inert pyrolysis ( $575 \text{ }^\circ\text{C}$ ).
- Tar cracking in the char bed zone, where heterogeneous and homogeneous reactions on the surface of the char take place.

Naturally, such cracking reactions are effective only if temperature and residence time of tars are high enough. Here, the residence time of tars in the oxidation and char zones bed was about three seconds, and temperatures varied between  $650 \text{ }^\circ\text{C}$  and  $700 \text{ }^\circ\text{C}$ . Previous studies have shown that above  $500 \text{ }^\circ\text{C}$  and with a residence time of tar around 2–3 s, heterogeneous cracking reactions of tars are significant and result in a higher yield of permanent gases and a lower yield of condensable vapors [15,22].

Finally, Fig. 6 shows that the yield of pyrolysis water was higher here (25 wt% for an air flux of  $0.022 \text{ kg m}^{-2} \text{ s}^{-1}$ ) than during inert allothermal pyrolysis (15 wt%). This can be attributed to oxidation and/or cracking reactions in the oxidation zone and char bed zone.

### 3.2. Product analyses

In this section, the analyses of the products from the experiments with wood chips and an air flux of  $0.022 \text{ kg m}^{-2} \text{ s}^{-1}$  are detailed.

#### 3.2.1. Char

The results of ultimate and proximate analyses of the char produced during the experiment are summarized in Table 3. The resulting char contained more than 94% of carbon.

Volatile matter (VM) content of chars is of particular interest for gasifier optimization. As the char produced during pyrolysis is gasified in the subsequent step of the process, it is extremely important

Table 3

Proximate and ultimate analysis of the char produced during the experiment with wood chips and an air flux of  $0.022 \text{ kg m}^{-2} \text{ s}^{-1}$ .

Proximate analysis (wt%, d.b)	
Ash	$1.2 \pm 0.2$
Volatile matter	$4.2 \pm 0.5$
Fixed carbon	$94.6 \pm 0.7$
Ultimate analysis (wt%, d.b.)	
C	$94.9 \pm 0.5$
H	$1.9 \pm 0.25$
N	$0.55 \pm 0.05$
O (by difference)	$2.65 \pm 0.75$
LHV (MJ/kg, d.b.)	$34 \pm 0.12$

that the VM content remains as low as possible in order to avoid the release of organic compounds in the syngas. From this point of view, the char produced by oxidative pyrolysis is of particular interest. The main reason is the higher temperature reached during pyrolysis due to in-situ oxidation. Indeed, a previous study by the same authors [15] showed that the influence of the oxidation reaction on char quality was not significant and that the temperature was the parameter that had the most influence. This low VM content is also responsible for the high LHV measured on the resulting char.

#### 3.2.2. Permanent gases

The mass yields of permanent gases during the experiment are presented in Fig. 6. The composition of the gas calculated on the basis of dry wood was 31.8%  $\text{CO}_2$ , 22.8%  $\text{CO}$ , 1.3%  $\text{H}_2$ , 3%  $\text{CH}_4$ , 1%  $\text{C}_2\text{H}_4$ , and 0.4%  $\text{C}_2\text{H}_6$ . The yields of  $\text{CO}$ ,  $\text{CO}_2$ , and  $\text{H}_2$  measured during oxidative pyrolysis were higher than those measured during inert pyrolysis [15,23].

On a permanent gas volume basis (including nitrogen), the composition of the gases at the outlet was 47.5%  $\text{N}_2$ , 15.8%  $\text{CO}_2$ , 17.6%  $\text{CO}$ , 13.8%  $\text{H}_2$ , 4.1%  $\text{CH}_4$ , 0.9%  $\text{C}_2\text{H}_4$ , and 0.3%  $\text{C}_2\text{H}_6$ .

#### 3.2.3. Tars

To date, several definitions of tars can be found in the literature [24]. Tars are composed of hundreds of condensable organic compounds. Today, it is not possible to identify and to quantify all the molecules because many of them are only present in trace amounts. Devi et al. [23] defined tars as a complex mixture of condensable hydrocarbons, containing one to several aromatic rings and other oxygenates and polycyclic aromatic hydrocarbons (PAHs). Tars are very frequently classified in three categories [24–28]:

- Primary products: cellulose-derived products, hemicellulose-derived products and lignin-derived products (levoglucosan, hydroxyacetaldehyde, furfurals, methoxyphenols). These tars are produced at low temperatures (400–500 °C) with a short residence time.
- Secondary products: phenolics and olefins. These products are produced at moderate temperatures (600–700 °C) with a medium residence time.
- Tertiary products: methyl derivatives of aromatics (methyl acenaphthylene, methylnaphthalene, toluene and indene), and polycyclic aromatic hydrocarbons (PAHs) (benzene, pyrene, naphthalene, acenaphthylene, anthracene, phenanthrene). These tars are produced at high temperatures (800–900 °C) with a longer residence time.

More than 70 organic compounds were identified and quantified using the GC–MS. Despite our team’s experience in condensate analysis, only about 40 wt% of the organic condensates were quantified in the collected samples. This can be due to the existence of a huge number of minor compounds that are either co-eluted with similar molecules, or present at too low concentrations to be isolated in the chromatograph. Furthermore, pyrolytic lignin can be present in the sampled tars and is not quantified by chromatography. Dufour et al. [28] obtained similar results by quantifying up to 40 species in the pyrolysis condensates produced in a batch fixed-bed reactor. These species represented 40 and 43 wt% of the organic condensates produced at final temperatures of 325 °C and 625 °C respectively.

Condensates from oxidative pyrolysis of wood chips are listed in Fig. 7. Some quantified compounds were grouped in the following chemical families: phenols, guaiacols, furans, and PAHs. They are shown as a percentage of the mass of the dry wood chips. From the detected organic compounds in the tars, we observed that 57 wt% of them belong to primary group and the rest, 43 wt%, belong to secondary and tertiary groups. Compared with the literature [29,30], the majority of the organic compounds detected in inert atmosphere belong to the group of primary tars when they are extracted directly after the devolatilization of the biomass. For example, Milhé et al. [15] found that for inert pyrolysis at 475 °C, more than 98 wt% of the detected tars belong to primary group. We can thus confirm the occurrence of tar cracking and oxidation reactions during our experiments, resulting in more secondary tars and fewer primary tars than during inert pyrolysis. It is noteworthy that tertiary tars (PAHs), the most stable, accounted only for a minor part. This is due to the temperature (<800 °C) in

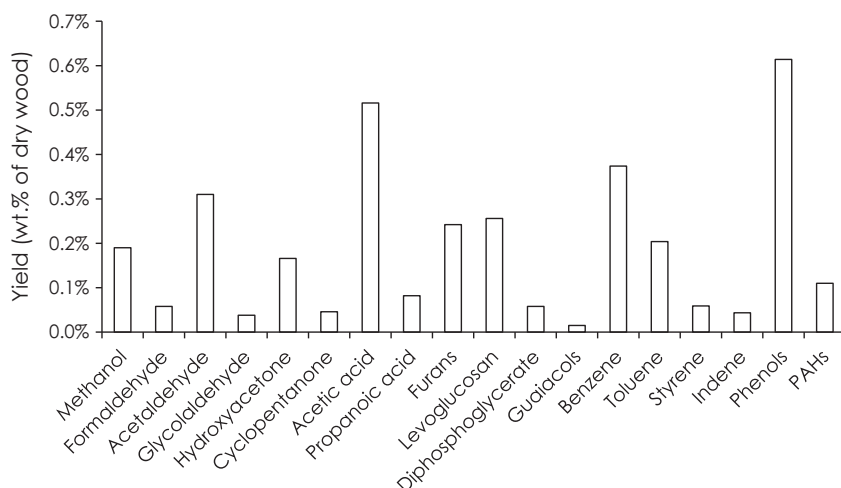


Fig. 7. Yields of organic condensates produced during the experiment with wood chips and an air flux of 0.022 kg m<sup>-2</sup> s<sup>-1</sup>.

the bed that does not allow the formation of heavier tertiary aromatics.

### 3.3. Effect of air flux

As mentioned above, air flux is known to be the most influential parameter in the front propagation rate. Indeed, the literature on reverse smoldering [13,16,17], cited three different regimes, depending on the main process controlling the propagation: oxygen-limited, reaction limited and quenching by convection. These regimes are clearly illustrated in Fig. 8 by the plot of wood chip flux versus air flux from the study of Porteiro et al. [13]. First there was a linear increase in the fuel flux with an increase in the air flux. Next, in the second zone, variations in the air flux did not influence the wood flux. Last, beyond a certain air flux, the wood flux decreased significantly until extinction of the front due to cooling of the reaction front by convective heat transfers.

The influence of air flux on the wood flux was investigated using both wood chips and wood pellets. Three air fluxes were tested: 0.014 kg m<sup>-2</sup> s<sup>-1</sup>, 0.022 kg m<sup>-2</sup> s<sup>-1</sup>, and 0.029 kg m<sup>-2</sup> s<sup>-1</sup>. Fig. 9 shows the results in terms of the wood flux as a function of air flux. Fig. 8 [13] shows that our study was in the oxygen-limited regime as the relation between the wood and air mass fluxes was almost linear. In industrial applications, smoldering regime must be in the oxygen-limited zone in order to control

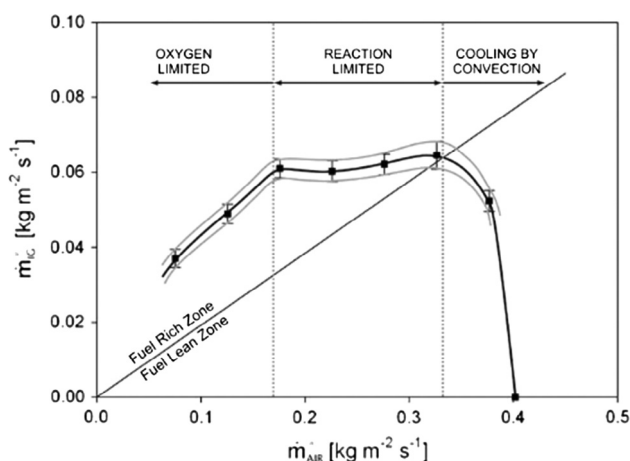
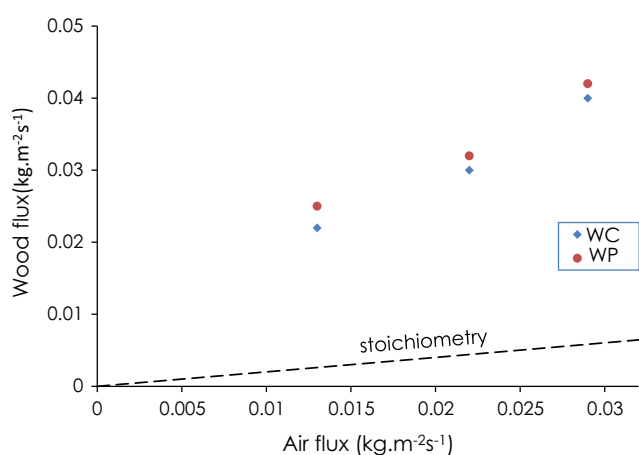


Fig. 8. The different regimes of smoldering relative to the air: wood ratio [13].





**Fig. 9.** Wood flux as a function of air flux for the two types of wood, wood chips (WC) and wood pellets (WP). Dashed line is for stoichiometry condition.

the input fuel power of the process by a simple regulation of the air flux.

The air: wood mass ratio is an essential parameter for process operation and optimization. With wood chips, this ratio was 0.61, 0.73, and 0.73 for air fluxes of 0.014, 0.022 and 0.029 kg m<sup>-2</sup> s<sup>-1</sup> respectively (Table 4). With wood pellets, the ratio was respectively 0.54, 0.68, and 0.67 for the three air fluxes considered. These results show that these ratios were lower with the low air flux, and remained constant with the two higher air fluxes. Thus, it appears that less air is consumed for a given progress of the oxidation zone when the injected air flux is low. The lower temperatures measured in that case may lower the oxidation kinetics and could be a first explanation. But comprehensive understanding cannot be stated only based on this experimental study. Indeed the progress of the oxidation zone is controlled by many phenomena, including chemical reactions, mechanical compaction, heat and mass transfers. Only a modelling approach to separate the impact of each phenomenon could provide answers. Nevertheless, the air: wood mass ratios were all between 0.54 and 0.73 in our operating conditions. Given that in stoichiometric conditions, this ratio is about 5.4 kg/kg, we can conclude that in our autothermal experiments, the oxidation zone consumes between 10% and 13.5% of the stoichiometric air to convert wood into char and gas.

Regarding the distribution of the products leaving the reactor, char yields decreased with an increase in the air flux. As can be

seen in Table 4, increasing the air flux from 0.014 to 0.029 kg m<sup>-2</sup> s<sup>-1</sup> char reduced the yield from 19.8% to 16.3%, for wood chips, and from 20.9% to 16.5% for wood pellets. The char yield in wood pyrolysis depends on many factors [31]. The most important factors in our case are the heating rate and the final temperature.

Table 4 also shows that the higher the air flux, the higher the temperature of the OZ: it increased by about 100 °C when the air flux was increased from 0.014 to 0.029 kg m<sup>-2</sup> s<sup>-1</sup>. Anca-Couce [31] showed that higher temperatures achieved in the reactor reduce the char yield. Moreover, it is likely that the rising in temperature and the acceleration of the OZ observed tend to increase the wood heating rate, which is also known to lower the char yield [28].

### 3.4. Effect of wood bulk density

The effect of wood density was investigated by comparing wood chips (WC) and wood pellets (WP). These two most common types of processed wood differ significantly in their bulk densities: 220 kg/m<sup>3</sup> for WC and 690 kg/m<sup>3</sup> for WP, i.e. a ratio of more than 3.

In the previous section (Fig. 9), it was shown that, despite the marked difference in the two wood densities, the difference in the air: wood ratio between wood chips and wood pellets is not so high. The yield distribution of the products of the two types of wood (Table 4) was also similar, except for water and some permanent gases yields (mainly CO, CO<sub>2</sub>, CH<sub>4</sub>, and H<sub>2</sub>) whatever the air flux used. For the same air flux, the temperatures in the reactor were higher with WP than with WC. For example, with an air flux of 0.022 kg m<sup>-2</sup> s<sup>-1</sup>, the mean OZ temperature was 680 and 700 °C respectively for WC and WP. This could be attributed to the structure of the OZ which depends on wood density. This temperature difference between WC and WP affects directly the kinetics of many reactions involved during pyrolysis, char gasification, oxidation (of wood, char, gas and tars), and water-shift. Thus, further explanation on the correlation between OZ temperature and yields of gases and water would require a detailed modelling approach.

The main difference between wood chips and wood pellets in the experiments was the upward velocity of the oxidation zone, which was much higher with wood chips than with wood pellets. We calculated the velocity of the oxidation zone during our experiment from the measurement of the wood mass flux and the wood bulk density as follows:

$$v_{OZ} = \frac{\phi_w}{\rho_w} \quad (4)$$

**Table 4**

Air: wood ratio, OZ temperature, and product yields for the two types of wood and three different air fluxes.

Air flux (kg m <sup>-2</sup> s <sup>-1</sup> )		0.014		0.022		0.029	
		WC	WP	WC	WP	WC	WP
Wood type		WC	WP	WC	WP	WC	WP
Air: wood mass ratio		0.61	0.54	0.73	0.54	0.73	0.54
Mean OZ temperature in T7 (°C)		600	650	680	700	730	730
Yields (wt% related to dry wood)							
Inlets							
	Dry wood		100	100	100	100	100
	Oxygen	14.26	12.67	17.27	16.05	17.21	15.87
	Total	114.3	112.7	117.3	116.1	117.2	115.9
Outlets							
	Permanent gases	CO <sub>2</sub>	26.36	30.46	31.77	36.21	32.76
		CO	21.31	16.26	22.80	15.92	17.79
		CH <sub>4</sub>	2.90	3.05	3.04	3.33	2.90
		H <sub>2</sub>	0.83	1.12	1.26	1.60	1.40
		C <sub>2</sub> H <sub>4</sub>	0.65	0.75	1.08	1.16	1.14
		C <sub>2</sub> H <sub>6</sub>	0.49	0.48	0.42	0.44	0.36
	Water	27.51	20.84	25.10	19.00	22.32	16.90
	Char	19.77	20.89	17.23	18.23	16.26	16.49
	Tars	10.02	11.62	8.48	9.01	11.33	7.43
	Total	109.8	105.5	111.2	104.9	106.3	108.2

where  $\phi_w$  [ $\text{kg m}^{-2} \text{s}^{-1}$ ] is the wood mass flux and  $\rho_w$  [ $\text{kg/m}^3$ ] is the wood bulk density.

The oxidation zone velocity was inversely proportional to the wood bulk density. This was to be expected since we obtained the same wood mass flux with wood chip and wood pellet feedstocks. For example, with an inlet air flux of  $0.022 \text{ kg m}^{-2} \text{ s}^{-1}$ , the oxidation zone velocity was  $0.82 \text{ cm/min}$  for wood chips and  $0.26 \text{ cm/min}$  for wood pellets. The same results have been reported by other authors who studied the effect of density on the velocity of oxidation zone in batch mode reactors [8,11].

Concerning the practical operation of the reactor, it should be noted that maintaining the oxidation zone at a fixed bed elevation using temperature measurements is more difficult with low density wood chips than with high density wood pellets. This can be explained by the differences in the structure of the oxidation zone with these two feedstocks, as discussed in the following section.

### 3.5. Structure of the oxidation zone

Information on the physical structure of the oxidation zone (OZ) during the experiments was obtained thanks to the measurements recorded by the eight thermocouples installed around the wall of the reactor at the same elevation as the OZ (i.e. 30 cm from the bottom grate). Figs. 10 and 11 show changes in the temperature over

time during experiments in continuous mode, for wood chips and wood pellets. The temperatures fluctuate because the OZ oscillates downward when extracting the char from the bottom of the reactor and upward due to its propagation towards virgin wood. The repeatability of the measurements throughout the different cycles of the experiments remained good. It is noteworthy that temperatures around the OZ were much more dispersed in the case of wood chips, where temperature differences of more than  $100 \text{ }^\circ\text{C}$  were measured. These results are confirmed by Fig. 12, which shows wall temperatures around the OZ at a fixed time (357 min for wood chips and 285 min for wood pellets) after char was extracted, when the temperatures were at their lowest. Figs. 10–12 clearly show that with wood chips the oxidation zone was not horizontal, whereas with wood pellets, the differences between the wall temperatures were very slight, meaning the oxidation zone was horizontal. A probable explanation of this difference in behavior is that solid flow is more uniform with wood pellets and is comparable with a piston flow due to high gravity force. The heterogeneous size and shape of wood chip particles results in a non-homogeneous flow of the reacting particle in the reactor, explaining why the shape of the OZ in a continuous operating mode is not flat. This is also why maintaining the oxidation zone at a fixed elevation in the reactor, based on bed temperature measurements, as mentioned previously, is more difficult with wood chips than with wood pellets.

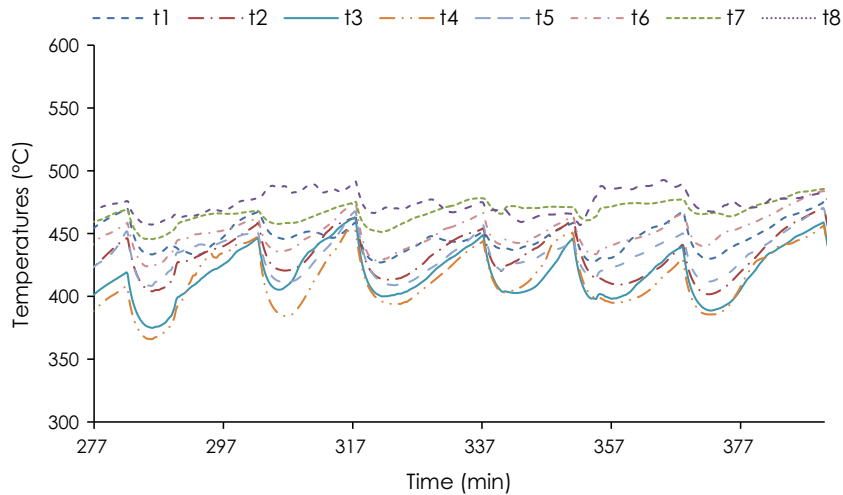


Fig. 10. Changes in temperatures around a section near the oxidation zone during the experiment with wood chips.

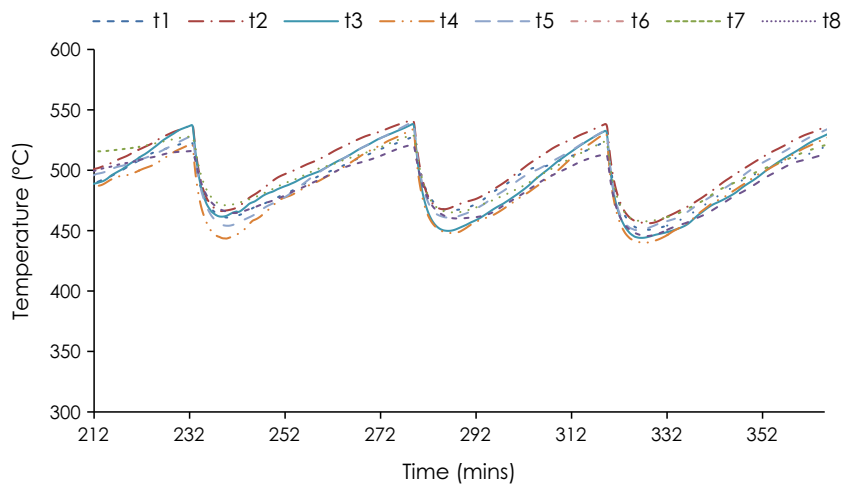


Fig. 11. Changes in temperature around a section near the oxidation zone during the experiment with wood pellets.

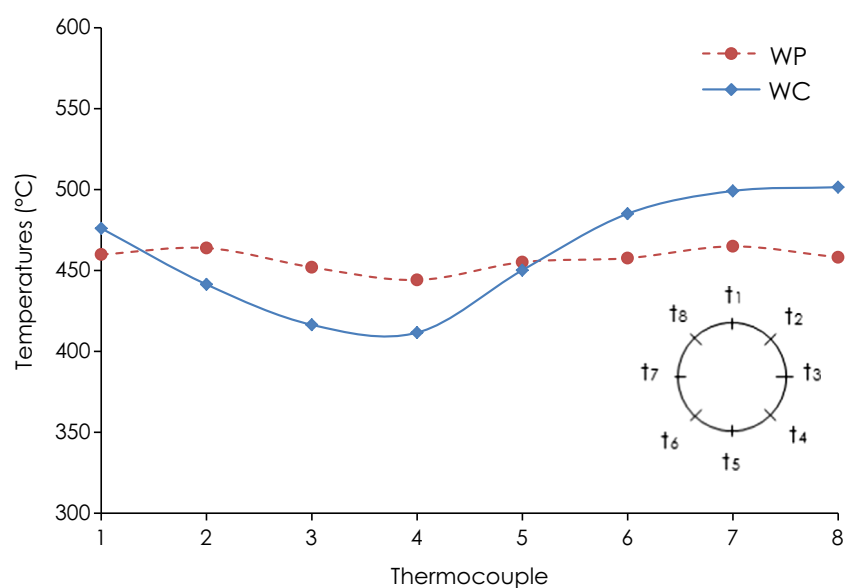


Fig. 12. Wall temperature profiles around a section near the oxidation zone during two experiments, the first with wood chips (WC), and the second with wood pellets (WP).

A new insight is proposed here to better interpret the observed air: wood mass ratios. In the literature, the air: wood mass ratio in a batch reactor in an oxygen limited zone is always higher than 1.5 [12–17]. In some experiments we conducted in batch mode (not shown in this paper) we observed ratios higher than 1.3. In continuous mode, this ratio was around 0.7. This means that the oxidation zone velocity is much higher in the continuous mode studied here than in batch modes. The explanation we propose is that in the batch mode studies, the reactor is initially at ambient temperature, and when OZ propagates inside a cold reactor, the transfer of heat from the OZ to the reactor wall is very intense, which slows down the propagation of the oxidation zone. In continuous mode, once the steady state regime is reached, the OZ remains in a preheated reactor zone, and the transfer of heat between the OZ and the wall is very low.

#### 4. Conclusion

The aim of this work was to investigate the behavior of oxidative autothermal pyrolysis of wood in a downdraft continuous fixed bed reactor. This mode of operation consists in maintaining a stable oxidation zone (OZ) inside the bed. The zone tends to propagate upward - opposed to wood and air flows - but can be kept at a fixed elevation by removing char at the bottom.

Such operating conditions were achieved using temperature measurement as an indicator of the elevation of the front. In a 20 cm I.D. insulated reactor, the resulting air: wood mass ratio of 0.7 was measured using an air flux in the range of 0.014–0.029 kg m<sup>-2</sup> s<sup>-1</sup>. The propagation of the oxidation zone consumes about 12% of the stoichiometric combustion air to provide energy for the autothermal pyrolysis process.

In stable continuous fixed bed conditions, oxidative pyrolysis of woodchips produced about 17% char, 10% tars, 25% water, and 55% permanent gases. This distribution differed slightly from that obtained with wood pellets, except for water yields. Air flux was shown to mainly affect char yield: a decrease of about 20% was measured when the air flux was doubled.

Overall, the air: wood ratio measured in our continuous operating mode was only slightly influenced by wood bulk density and air flux. But it is noteworthy that this ratio is 2–4 times lower than the ratios reported in batch mode experiments. In our opinion, this

underlines the importance of heat losses in the smoldering process as well as the advantage of the continuous pyrolysis process to optimize thermal efficiency.

Wood density was shown to significantly influence the velocity and the shape of the oxidation zone. Velocity was inversely proportional to the wood bulk density. In a bed made from dense wood pellets, the oxidation zone is almost flat and horizontal, whereas when wood chips are used, it is somewhat inclined. These results are linked to the impact of wood properties on particles flowing along the fixed bed, i.e. “piston” type for dense wood pellets, less homogenous and faster for wood chips.

This work was carried out using two wood samples both with about 9% moisture content. Future work will focus on the impact of this parameter on the behavior of the front.

#### Acknowledgements

This research was partly funded by CIRAD (French agricultural research center) and Mines-Nantes (French graduated school of engineering), in collaboration with Mines-Albi.

#### References

- [1] Antal MJ, Grønli M. The art, science, and technology of charcoal production. *Ind. Eng. Chem. Res.* 2003;42(8):1619–40.
- [2] Handbook biomass gasification. Biomass technology group (BTG). The Netherlands: Knoef HAM; 2012.
- [3] Anca-Couce A, Zobel N, Berger A, Behrendt F. Smoldering of pine wood: kinetics and reaction heats. *Combust Flame* 2012;159(4):1708–19.
- [4] de Souza Costa F, Sandberg D. Mathematical model of a smoldering log. *Combust Flame* 2004;139(3):227–38.
- [5] Carvalho ER, Gurgel Veras CA, CarvalhoJR JA. Experimental investigation of smoldering in biomass. *Biomass Bioenergy* 2002;22(4):283–94.
- [6] Ohlemiller TJ. Modeling of smoldering combustion propagation. *Prog Energy Combust Sci* 1985;11(4):277–310.
- [7] Nolter MA, Vice DH. Looking back at the Centralia coal fire: a synopsis of its present status. *Int J Coal Geol* 2004;59(1–2):99–106.
- [8] Martins MF, Salvador S, Thovert J-F, Debenest G. Co-current combustion of oil shale - Part 2: Structure of the combustion front. *Fuel* 2010;89(1):133–43.
- [9] Yang YB, Phan AN, Ryu C, Sharifi V, Swithenbank J. Mathematical modelling of slow pyrolysis of segregated solid wastes in a packed-bed pyrolyser. *Fuel* 2007;86(1–2):169–80.
- [10] Yang YB, Sharifi VN, Swithenbank J. Effect of air flow rate and fuel moisture on the burning behaviours of biomass and simulated municipal solid wastes in packed beds. *Fuel* 2004;83(11–12):1553–62.
- [11] Rostami A, Murthy J, Hajaligol M. Modeling of a smoldering cigarette. *J Anal Appl Pyrolysis* Jan. 2003;66(1–2):281–301.

- [12] Mahapatra S, Dasappa S. Experiments and analysis of propagation front under gasification regimes in a packed bed. *Fuel Process Technol* 2014;121:83–90.
- [13] Porteiro J, Patiño D, Collazo J, Granada E, Moran J, Miguez JL. Experimental analysis of the ignition front propagation of several biomass fuels in a fixed-bed combustor. *Fuel* 2010;89(1):26–35.
- [14] Porteiro J, Patiño D, Miguez JL, Granada E, Moran J, Collazo J. Study of the reaction front thickness in a counter-current fixed-bed combustor of a pelletised biomass. *Combust Flame* 2012;159(3):1296–302.
- [15] Milhé M, van de Steene L, Haube M, Commandré J-M, Fassinou W-F, Flamant G. Autothermal and allothermal pyrolysis in a continuous fixed bed reactor. *J Anal Appl Pyrolysis* 2013;103:102–11.
- [16] Ryu C, Yang YB, Khor A, Yates NE, Sharifi VN, Swithenbank J. Effect of fuel properties on biomass combustion: Part I. Experiments—fuel type, equivalence ratio and particle size. *Fuel* 2006;85(7–8):1039–46.
- [17] Shin D, Choi S. The combustion of simulated waste particles in a fixed bed. *Combust Flame* 2000;121(1–2):167–80.
- [18] Saastamoinen JJ, Taipale R, Horttanainen M, Sarkomaa P. Propagation of the ignition front in beds of wood particles. *Combust Flame* 2000;123(1–2):214–26.
- [19] Teixeira G. Gazéification de charbon de granules de bois : comportement thermo-chimique et mécanique d'un lit fixe continu. Toulouse, INPT; 2012.
- [20] Mermoud F. Gazéification de charbon de bois à la vapeur d'eau : de la particule isolée au lit fixe continu. Toulouse, INPT; 2006.
- [21] Van de steene L, Tagutchou JP, Escudero Sanz FJ, Salvador S. Gasification of woodchip particles: experimental and numerical study of char-H<sub>2</sub>O, char-CO<sub>2</sub>, and char-O<sub>2</sub> reactions. *Chem Eng Sci* 2011;66(20):4499–509.
- [22] Anis S, Zainal ZA. Tar reduction in biomass producer gas via mechanical, catalytic and thermal methods: a review. *Renew Sustain Energy Rev* 2011;15(5):2355–77.
- [23] Devi L, Ptasinski KJ, Janssen FJJG, van Paasen SVB, Bergman PCA, Kiel JHA. Catalytic decomposition of biomass tars: use of dolomite and untreated olivine. *Renew Energy* 2005;30(4):565–87.
- [24] Devi L, Ptasinski KJ, Janssen FJJG. A review of the primary measures for tar elimination in biomass gasification processes. *Biomass Bioenergy* 2003;24(2):125–40.
- [25] Han J, Kim H. The reduction and control technology of tar during biomass gasification/pyrolysis: an overview. *Renew Sustain Energy Rev* 2008;12(2):397–416.
- [26] Li C, Suzuki K. Tar property, analysis, reforming mechanism and model for biomass gasification—an overview. *Renew Sustain Energy Rev* 2009;13(3):594–604.
- [27] Elliott DC. Relation of reaction time and temperature to chemical composition of pyrolysis oils. *Pyrolysis oils from biomass*. American Chemical Society; 1988. p. 55–65. vol. 376, 0 vols.
- [28] Dufour A, Girods P, Masson E, Normand S, Rogeaume Y, Zoulalian A. Comparison of two methods of measuring wood pyrolysis tar. *J Chromatogr A* 2007;1164(1–2):240–7.
- [29] Boroson ML, Howard JB, Longwell JP, Peters WA. Product yields and kinetics from the vapor phase cracking of wood pyrolysis tars. *AIChE J Jan.* 1989;35(1):120–8.
- [30] Baumlin S, Broust F, Ferrer M, Meunier N, Marty E, Lédé J. The continuous self stirred tank reactor: measurement of the cracking kinetics of biomass pyrolysis vapours. *Chem Eng Sci Jan.* 2005;60(1):41–55.
- [31] Anca-Couce A. Reaction mechanisms and multi-scale modelling of lignocellulosic biomass pyrolysis. *Prog Energy Combust Sci* 2016;53:41–79.